






Project Number 101061230

# **DELIVERABLE D3.2** **REPORT ON METAL TARGETS** **AND ASSOCIATED DISSOLUTION STRATEGY**

**Lead Beneficiary: SCK CEN**

Due date: 31/03/2024

Released on: 27/03/2023

Authors:	Andrew Cea Dennis Elema	
Version:	1.2	
For the Lead Beneficiary	Reviewed by Work package Leader	Approved by Coordinator
Andrew Cea	Renata Mikołajczak	Renata Mikołajczak
	 Kierownik Projektu Prof. dr hab.inż. Renata Mikołajczak	 Kierownik Projektu Prof. dr hab.inż. Renata Mikołajczak

Dissemination Level		
PU	Public	X
RE	Restricted to a group specified by the Beneficiaries of the SECURE	
CO	Confidential, only for Beneficiaries of the SECURE project	

### Version control table

Version number	Date of issue	Author(s)	Brief description of changes made
1.0	23/03/2024	Andrew Cea	1 <sup>st</sup> draft
1.1	25/03/2024	Michaela Velckova	Reviewed by MST, formal check
1.2	27/03/2024	Renata Mikołajczak, Andrew Cea	Last revision, comments Final version

### Project information

Project number:	101061230
Project full title:	Strengthening the European Chain of supply for next generation medical Radionuclides
Acronym:	SECURE
Call and topic:	HORIZON-EURATOM-2021-NRT-01-10
Type of action:	EURATOM-RIA
Project Coordinator Organization:	NCBJ
Coordinator:	Renata Mikołajczak
EC Project Officer:	Renata Bachorczyk-Nagy
Start date – End date:	01/10/22 – 30/09/25 (36 months)
Coordinator contact:	Renata.Mikolajczak@polatom.pl
Administrative contact:	+420 245 008 599, <a href="mailto:jakub.heller@evalion.cz">jakub.heller@evalion.cz</a>
Online contacts (website):	<a href="https://enen.eu/index.php/portfolio/secure-project/">https://enen.eu/index.php/portfolio/secure-project/</a>

### Copyright

The document is proprietary of the SECURE consortium members. No copying or distributing, in any form or by any means, is allowed without the prior written agreement of the owner of the property rights. This document reflects only the authors' view. The European Commission is not liable for any use that may be made of the information contained herein.

Funded by the European Union. Views and opinions expressed are however those of the author(s) only and do not necessarily reflect those of the European Union or the European Commission. Neither the European Union nor the European Commission can be held responsible for them.



Funded by the  
European Union

## EXECUTIVE SUMMARY

The production and dissolution of W-186 metal targets were investigated. A W-186 target undergoes a double-neutron capture to produce W-188, a beta-emitting isotope used in nuclear medicine. Its daughter nuclide Re-188, decays and is accompanied by a 155 keV predominant energy  $\gamma$ -emission, which could be used for  $\gamma$ -cameras, for imaging, biodistribution, or absorbed radiation dose studies. Additionally, its high beta emissions can penetrate and destroy abnormal tissue or cancer for therapy.

Both oxide and metallic W-186 have been reported in the literature [2]. Oxide targets are preferred for the ability to dissolve and retrieve the W-186 product after irradiation. However, the ampoules of tungsten oxide targets have been reported to break, limiting the possibility of upscaling. Additionally, the lower W-density in the oxide form is unfavourable, given that there is limited availability in high-flux positions in research reactors. Although it is unclear why these ampoules break, a working hypothesis presumes it is due to the heat generated, the low thermal conductivity, and the thermal expansion of the material during irradiation. Therefore, W-metal targets are investigated to improve target performance during irradiation and increase production per irradiation cycle.

In this report, a feasibility study of W-metal targets was performed by making and dissolving W-metal target samples. Various metal targets were made by pressing, sintering, and cutting W-powder. The die and punch had a cylindrical cavity with a diameter of 9.8mm. The applied force varied from sample to sample, from 4 to 6 tons in a hydraulic press. The samples were then sintered in a Hyptec 5 atmosphere at 1750°C for 2 and 24 hours. Following the production and characterization of these targets, they were then dissolved to study the time and conditions needed to extract medical isotopes.

To dissolve these targets, a single-step hydrogen peroxide method was used. The reaction was heated in a water bath up to 45°C and confirmed by weighing the residual W-mass. The reaction was observed to occur in three phases. Phase one - the initial dissolution phase occurred over the first 12 minutes, with small hydrogen bubble formation. In phase two, a vigorous reaction was present between 12 and 16 minutes, where the target fell apart into a powder. After 60 minutes, it was found that around 91% of the initial target was dissolved. In phase three, the dissolution of the residual W-mass proceeded slowly until the reaction was stopped at 90 minutes. At 90 minutes, the residual W-mass was found to be between 1-2% of the initial target mass.

# CONTENT

<b>1</b>	<b>INTRODUCTION .....</b>	<b>5</b>
1.1	TARGET TYPE.....	5
1.1.1	<i>Physical and chemical state</i> .....	5
1.1.2	<i>Target geometry</i> .....	5
1.2	DISSOLUTION STRATEGY .....	6
<b>2</b>	<b>MATERIALS AND METHODS.....</b>	<b>7</b>
2.1	STARTING MATERIAL .....	7
2.2	SCANNING ELECTRON MICROSCOPE .....	7
2.3	EQUIPMENT AND FABRICATION .....	8
2.3.1	<i>Pellet fabrication</i> .....	8
2.3.2	<i>Annealing</i> .....	8
2.3.3	<i>Cutting pellets into disks</i> .....	9
<b>3</b>	<b>RESULTS.....</b>	<b>10</b>
3.1	MICROSTRUCTURE AND POROSITY OF METAL TARGETS .....	10
3.1.1	<i>Porosity estimation</i> .....	10
3.1.2	<i>Characterisation of particle interfaces</i> .....	11
3.2	DISSOLUTION OF TARGETS IN PEROXIDE .....	12
<b>4</b>	<b>SUMMARY AND CONCLUSIONS .....</b>	<b>14</b>
4.1	SUMMARY AND DISCUSSION .....	14
4.2	RECOMMENDATIONS .....	14
<b>5</b>	<b>CITATION .....</b>	<b>15</b>

# 1 INTRODUCTION

## 1.1 Target type

### 1.1.1 Physical and chemical state

Metallic and enriched W-186 discs have been chosen as target material because the W-density of a solid metal target is much higher than W-oxide targets. This allows for larger amounts of W to be irradiated in the limited space available in the high flux positions, despite that the irradiation of loose powders gives higher specific activities than of solids due to the reduced self-shielding. Powder W-186 targets have been irradiated in BR2 in the past, however, the overall yields were too low. Furthermore, there is a higher contamination risk during the decanning of powders or during the manipulations of the chemical process in a hot cell. Similar processing risks have been reported by Oak Ridge National Laboratory [3]. Therefore, a compact solid form has been favoured over the powdered form.

### 1.1.2 Target geometry

Target geometries must be optimized for both irradiation conditions and dissolution conditions. For the optimization of W-188 production, the following parameters are considered:

- Global geometry – A cylindrical target is studied in this report. The majority of W targets that are irradiated in research reactors are cylindrical. In the case of W-188 production, tungsten is irradiated in a quartz ampoule with an aluminum can. To decrease the amount of thermal neutron self-shielding and optimize the amount of W188 activity produced/gram, it is important to keep the cylindrical height  $\leq$  radius of the cylinder [2]. In this report, a cylinder with a radius of 9.8mm and a height of 2mm is studied.

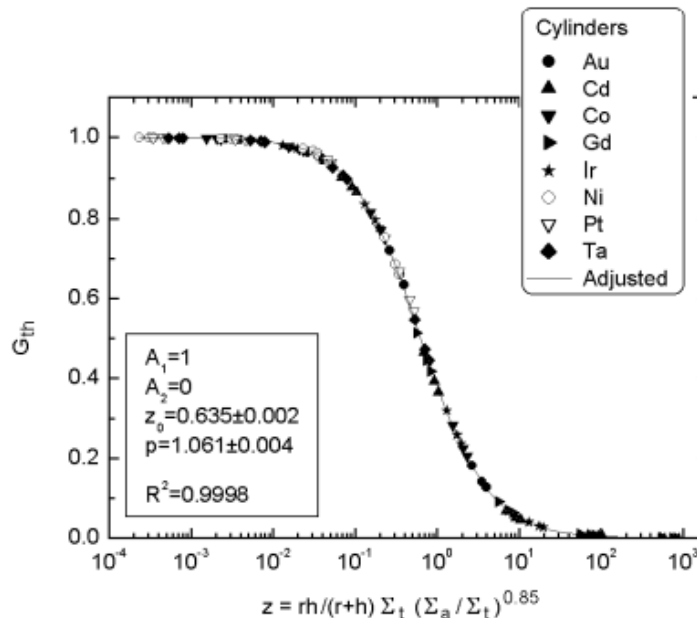


Figure 1. Thermal neutron self-shielding factor of cylindrical samples, where  $r$  and  $h$  are cylinder radius and height respectively[1].

- Macroscopic geometry – The targets should have meso- or macroscopic porosity. The increased surface area and decrease in density will help increase the available surface area to react in solution and decrease the self-shielding in the sample respectively. In this report, macroscopic porosity is created as a function of initial powder size and geometry, and low pressing and sintering conditions.
- Microstructure geometry – Considerations for microstructural optimization include grain size, grain boundary analysis, formation of precipitates, and other classical microstructural characteristics. For this study, only the quality of the particle-particle interfaces is investigated. As the production of these targets starts from powders, it is important to ensure that the particles are chemically bonded to each other at the end of the fabrication process and to minimize loose powder from breaking during and after irradiation.

## 1.2 Dissolution strategy

In reported literature, tungsten metal targets are first converted to tungsten oxide (commonly  $\text{WO}_3$ ) before any further chemical processing [1, 3, 4]. Tungsten metal is converted to  $\text{WO}_3$ , by heating the sample at  $750^\circ\text{C}$  in a quartz reaction vessel inside a furnace under a constant airflow. During heating, tungsten metal reacts with oxygen to form tungsten oxides ( $\text{WO}_3$ ) that are soluble in the follow-up dissolution in highly concentrated  $\text{NaOH}$ . This oxidation process also converts Os-188 and Os-191 into  $\text{OsO}_4$ , a highly volatile and toxic gas. In this process, the metal target is simultaneously transformed into a soluble oxide form and volatile  $\text{OsO}_4$  is removed from the solid  $\text{WO}_3$  product by airflow and absorbed by a scrubbing array.

There are two major disadvantages of the method. First, oxygen reacts with pure tungsten metal and not if tungsten is alloyed with other elements at high temperatures. The  $\text{O}_2$ -W reaction is retarded by WRe or WC formation on the surface of the irradiated W. Secondly, the formation of  $\text{OsO}_4$  in high yield ( $>90\%$ ) must be absorbed completely from the reaction of ( $\text{Os} + \text{O}_2$ ), and scrubbers are applied and optimized for safety.

To resolve both potential problems, the direct dissolution of the W metal target with peroxide is studied to avoid the heating step that generates a large amount of volatile  $\text{OsO}_4$ . This report demonstrates the time and characteristics of the dissolved target for optimized target processing.

## 2 MATERIALS AND METHODS

### 2.1 Starting Material

- Tungsten Powder

A tungsten powder with a natural isotopic abundance was used in this study. The powder was purchased from General Electric and was sieved with a mesh size -100 +325. The elemental purity is reported to be in percentage; W> 99.9, Al< 0.001, Ca < 0.0005, Co < 0.001, Cu< 0.0005, Fe < 0.0013, Mg < 0.0007, and other elements <0.001. The porosity after lab milling is reported to be 0.504. The particle size range is between 7 and 100 µm and is faceted and irregular.

- Peroxide

The peroxide used was purchased from Fisher Scientific. The solution was purely hydrogen peroxide 100 volumes 30-32% w/w, primary-trace analysis grade.

### 2.2 Scanning electron microscope

The SEM that is used in this work is a JEOL JSM 7100 LV, Field Emission Gun (FEG) SEM is installed and augmented with a Bruker EDS detector. The SEM is coupled to a stainless steel glovebox and mounted inside a concrete hot cell, allowing for the examination of radioactive specimens up to an activity of 4.44 MBq. Detailed specifications of the SEM can be found in Table.

**Table 1) JEOL JSM6610 characteristics**

#### **JEOL JSM6610 LV**

Filament	Schottky Field Emission Gun (FEG)
Acceleration Voltage	0.1 – 30 kV
Probe Current	1 pA – 200 nA
Magnification	x 10 – x 1 000 000
Stage	5-axes (X, Y,Z, R,T) mechanically eucentric stage
Max specimen size	Ø < 100 mm h < 40 mm
Max specimen weight	2 kg
Low Vacuum	Variable pressure: 10 – 300 Pa
Pixels	1280 x 960 – 5120 x 3840
Resolution High Vacuum	1.2 nm at 30 kV, WD 10 mm, secondary electrons 2 nm at 1 kV, WD 10 mm, secondary electrons
Resolution Low Vacuum	3 nm at 30 KV, WD 10 mm, 30 Pa backscattered electrons 3 nm at 30 KV, WD 10 mm, 60 Pa secondary electrons

## 2.3 Equipment and fabrication

### 2.3.1 Pellet fabrication

Punch press – The punch and die set to make the pellets are presented in Figure 2. The diameter of the set is 9.8mm. The set is made out of stainless steel. The ends of the punches are coated in tungsten carbide.

The W powder was pressed with an Atlas automatic 8 Ton hydraulic press, with the punch and die. The die was lubricated with saturated stearic acid in acetone.



Figure 2) Assembled Punch and die set - 9.8 diameter. The body is made of stainless steel. The ends are of the punches are made of tungsten carbide

### 2.3.2 Annealing

The resulting pellets were then sintered in a Linn HT-1800 Moly oven where the pellet is placed in an alumina boat and heated at a rate of 5 K.min<sup>-1</sup> up to 1750°C. under a Hyptec 5 atmosphere. Three pellets were kept at 1750°C for 2 hours and 3 pellets were kept at for 24 hours. The resulting pellets are presented in Figure 3.

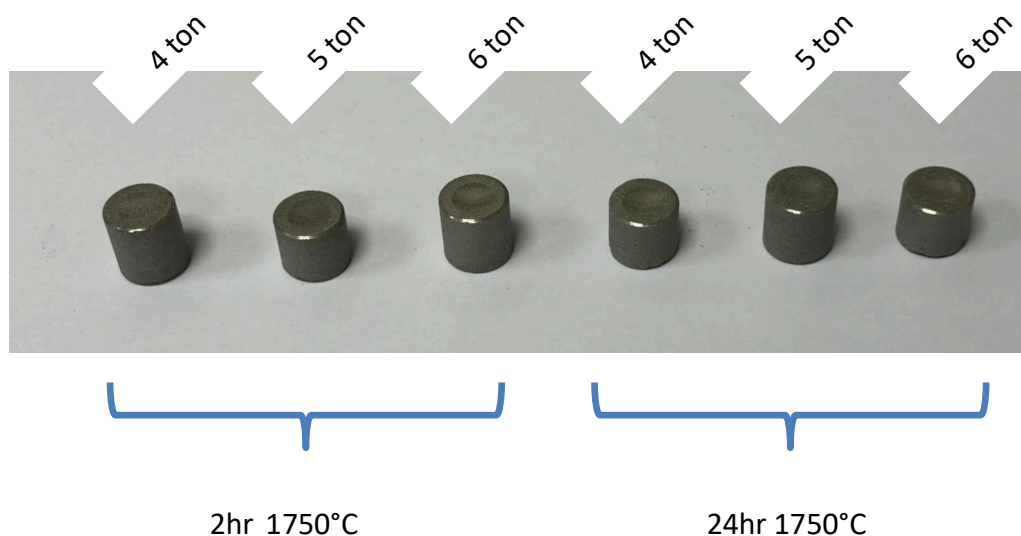
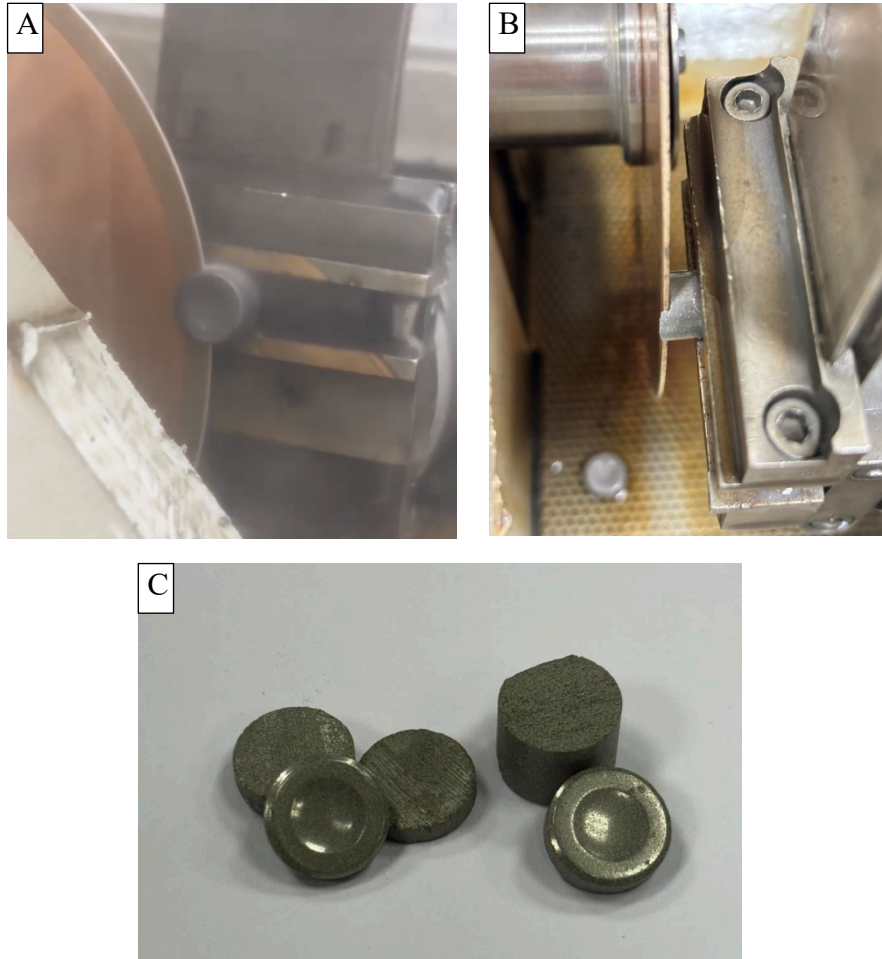


Figure 3) Pellets made from pressing and sintering tungsten powder. Different pressing conditions and sintering times are shown.



### 2.3.3 Cutting pellets into disks

The resulting pellets were then cut into disks for their final geometry. A Norton diamond wheel was used to cut the pellets in a Struers Accutom-50 cut-off machine (Figure 4A). The disks were measured with a digital point micrometre. The disks broke off prematurely (Figure 4B), resulting in a burr on the remaining pellet. The resulting disks were on average  $2.2 \pm 0.1 \mu\text{m}$  in thickness and did not show any further damage (Figure 4C) after fabrication.



**Figure 4) Disk preparation – A; Cutting with a diamond saw. B; Burr development after cutting. C; 2.2mm disks from a cut pellet.**

## 3 RESULTS

### 3.1 Microstructure and porosity of metal targets

#### 3.1.1 Porosity estimation

Pellets were analyzed with scanning electron microscopy. Both secondary and backscattered electron micrographs were taken to evaluate the quality of the pellet and the bonding of the powder after pressing and sintering.

For a comparative study, disks from two pellets have been characterized;

- Pellet A - W-pellet that was pressed under 4 tons, Ø9.8mm, and sintered for 2h at 1750°C in a Hyptec 5 atmosphere. Type A disks were cut from this pellet.
- Pellet B - W-pellet that was pressed under 6 tons, Ø9.8mm, and sintered for 24h at 1750°C in a Hyptec 5 atmosphere. Type B disks were cut from this pellet.

To estimate the total porosity, a combination of image analysis and He-pycnometry was used. For macropores or the global porosity of the pellet, SEM images were analysed through the program Sigma Scan Pro 5. Backscattered micrographs were used to estimate the porosity, as voids or pores are visible as different intensities due to the density contrast. For each disk and pellet, over 30 images were taken at random at 100x, 1000x and >1000x magnification. For each pellet, 20 He-pycnometry cycles were used to estimate the porosity of the continuous W-phase.

Examples of SEM micrographs are presented in Figure 5. In Figure 5A, a SE micrograph of a pellet pressed under 4 tons and sintered at 1750°C for 2 hours is shown. The pellet surface is shown to be rough and discontinuous. In Figure 5B, a BSE micrograph is presented of a pellet that has been pressed with 6 tons and annealed for 24 hours. The porosity of this pellet is demonstrated by the contrast in densities. Using only BSE images processed through Sigma Scan Pro 5, it is estimated that Pellet A has a global porosity of  $27\pm5\%$  and Pellet B is estimated to have a global porosity of  $20\pm2\%$ .

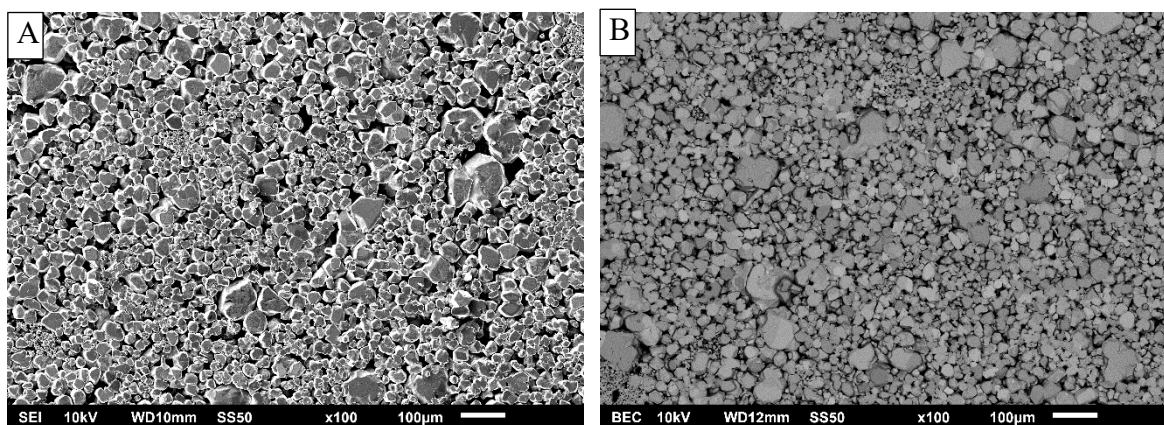


Figure 5) A; SE image of pellet pressed under 4 tons and sintered at 1750°C for 2hours. B; BSE image of pellet pressed under 6 tons and sintered at 1750°C for 24hours.

An AccuPyc II 1345 gas displacement pycnometer was used to estimate the porosity of the continuous W-phase. The sample is sealed in the instrument compartment of known volume, He gas is admitted and then expanded into another precision internal volume. A representative table is provided in Table 2 for pellet A. For the continuous tungsten phase, all 6 pellets were measured to have 99% theoretical density and almost no porosity.

**Table 2) He-pycnometry measurement data from Pellet A – Pressed under 4 tons and annealed for 24 hours.**

Cycle#	Volume (cm <sup>3</sup> )	Volume Deviation (cm <sup>3</sup> )	Density (g/cm <sup>3</sup> )	Density Deviation (g/cm <sup>3</sup> )	Elapsed Time (mm:ss)	Temp (°C)
1	0.6181	0.0000	19.2459	0.0000	7:28	25.57
2	0.6182	0.0000	19.2449	-0.0010	9:38	25.59
3	0.6159	-0.0023	19.3172	0.0713	11:56	25.60
4	0.6174	-0.0007	19.2692	0.0233	14:04	25.62
5	0.6182	0.0001	19.2435	-0.0024	16:37	25.65
19	0.6183	0.0002	19.2400	-0.0059	48:06	25.82
20	0.6184	0.0003	19.2380	-0.0079	50:26	25.81
Summary Data	Average	Standard Deviation				
Volume:	0.6181 cm <sup>3</sup>	0.0006 cm <sup>3</sup>				
Density g/cm <sup>3</sup>	19.2459	0.0195				

### 3.1.2 Characterisation of particle interfaces

Particle-particle interfaces were optimized and examined to evaluate the quality of the compact. The powder in the compacts must be sufficiently bonded to each other to ensure that the compact does not come loose during fabrication, irradiation, or decanning. However, increased pressing and sintering time/temperature will lead to a decrease in porosity. Therefore, this study of pressing and sintering conditions is to optimize the interfaces to ensure sufficient bonding, but also preserve the integrity of the pore structure.

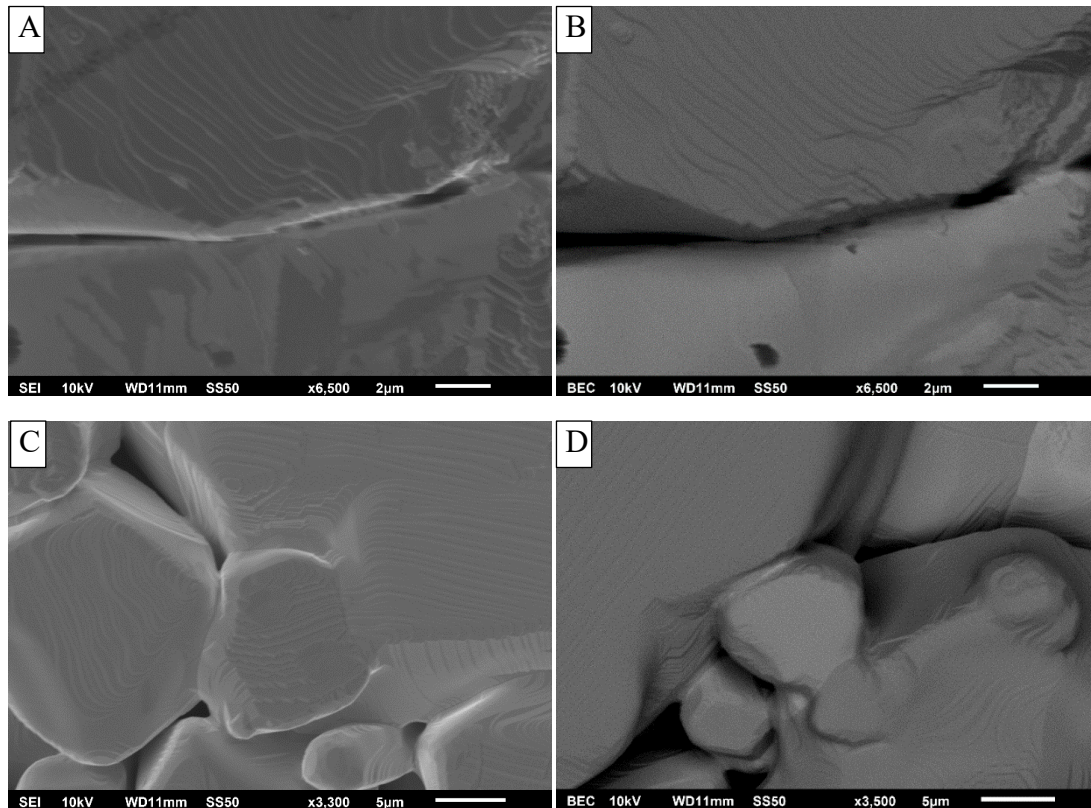


**Figure 6) SEM micrographs of pressed and sintered W-metal pellets. A and B; SE and BSE micrograph of 4ton pressed pellet sintered at 1750°C for 2hrs. C and D; SE and BSE micrograph of 6 ton pressed pellet sintered at 1750°C for 24 hrs. All images were taken with 10kV and at a working distance of 11mm.**

An example of micrographs of particle-particle interfaces is presented in Figure 6. Micrographs A and B are of pellet A – pressed at 4 tons, 9.8mmØ, and annealed for 2 hours in a Hyptec 5 atmosphere. The interfaces of the particles show a sharp decrease in density, indicating that the particles are not chemically bonded at the junction. The powder in this pellet was likely mechanically bonded due to pressing.

Micrographs in Figure 6 C and D, are of pellet B, pressed at 6 tons, 9.8mmØ, and annealed for 2 hours in a Hyptec 5 atmosphere. The interfaces of these pellets show similar densities as that of the bulk powder. The extended force and anneal time of these pellets were sufficient for chemically bonded interfaces.

### 3.2 Dissolution of targets in peroxide

As reviewed in section 1.2, hydrogen peroxide was used to dissolve W-metal targets. This strategy was chosen as a single-step dissolution strategy, to optimize the dissolution time and avoid heating Os vapors in the conversion of W -metal to  $WO_3$ . In this dissolution study, only targets cut from a pellet B were used. Pellet type A – made from a 4-ton press and 2 hours of annealing, did not show sufficient bonding to be safe for handling and decanning. Pellet type B was demonstrated to have sufficient bonding in the particle interfaces, and would be suitable for isotope production. Therefore, only Pellet B was studied further to assess its chemical performance. The pellet was cut into 2.2mm thick disks, hereafter referred to as a Type-B disk.

Six Type-B disks were dissolved in different conditions. The initial mass of the disk was recorded. For each disk, 15 ml of hydrogen peroxide was used in the initial phase. A beaker was placed in a water bath and heated to the reported temperature. The reactions were stopped at either 60 or 90 minutes. Residual tungsten was rinsed, dried, and weighed after each experiment.

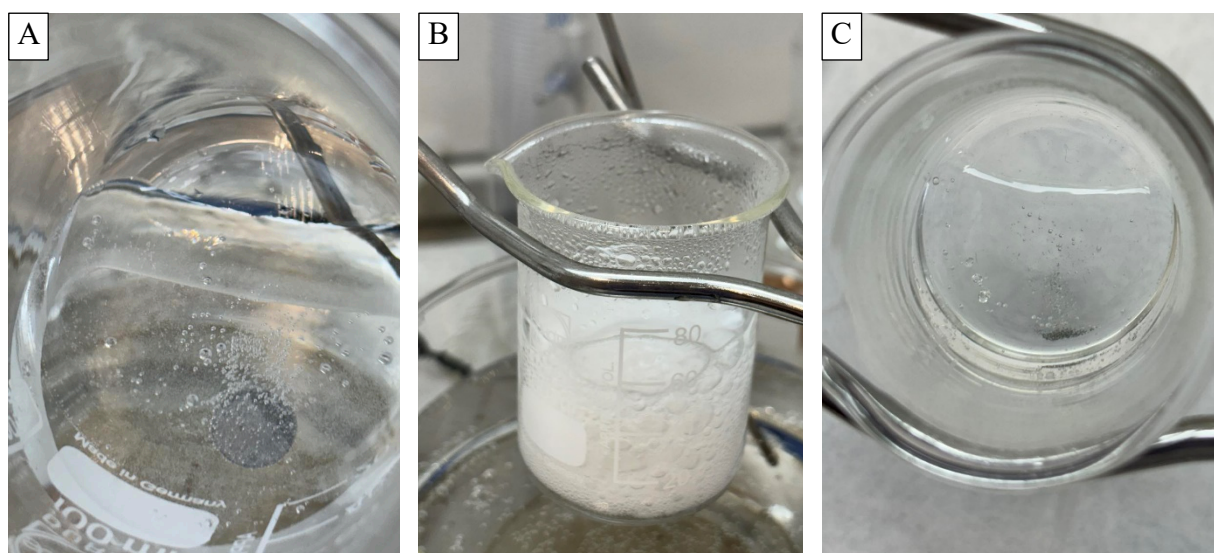


**Figure 7) 2.2mg W-metal target dissolved in hydrogen peroxide 30% w/w. Target pressed at 6 tons, 2h at 1750°C. A; stage 1 with small bubbles. B; Stage 2 with vigorous bubbling. C; stage 3 with residual tungsten mass.**

The results of the dissolution tests are recorded in Table 3 and shown in Figure 7. Type B disks dissolved in hydrogen peroxide showed three distinct stages. In stage one (Figure 7A) the disk produced small hydrogen bubbles as the reaction started. In stage two (Figure 7B) large bubbles were created. The target fell apart into a powder and the reaction proceeded vigorously. In stage three (Figure 7C) residual tungsten powder slowly dissolved. These stages of the dissolution process were found to be temperature-dependent. For experiments performed at 45°C (Tests 3-6, Table 3), the first stage would occur during the first 12 minutes. Stage two occurred in between 12 and 16 minutes. Finally, stage three lasted from 16 minutes to 90 minutes. In this final stage, an additional 10ml of peroxide was added. Although the majority of the target was dissolved in 60 minutes (Table 3, test 3), only an additional 7-9% of the target was dissolved for an additional 30 minutes. For experiments performed at room temperature, the targets did not reach stage two within 60 minutes.

**Table 3) Dissolution of Type-B disks. Time, initial mass, and residual mass was recorded for each experiment.**

Test no.	Temp. (°C)	Time (minutes)	Initial Target mass (g)	Residual mass (g)	% dissolved
1	22	60	2.23	1.3	41.7
2	22	90	2.22	0.94	57.6
3	45	60	2.22	0.20	91.0
4	45	90	2.09	0.03	98.5
5	45	90	2.15	0.04	98.2
6	45	90	2.22	0.04	98.2



## 4 SUMMARY AND CONCLUSIONS

### 4.1 Summary and Discussion

Reported here is a feasibility study on the production of tungsten metal targets and a dissolving method with hydrogen peroxide. The combined target production-dissolution strategy was designed to optimize the target performance during fabrication, during irradiation, and the extraction of isotopes afterwards. A combined study in isotope production helps support future producers of this isotope by eliminating pitfalls along the production pathway. Targets optimized for production and irradiation without a dissolution strategy risk production without a reasonable purification time. This problem is exemplified in production strategies revealing targets with a purification step larger than the half-life of the isotope, rendering the target-purification pair inefficient. Studies focus on purification without consideration of the target design risk an unrealistic dissolution or chemical separation strategy that may not work with all target types and microstructures, or may lead to incomplete chemical processing of the target.

In this study, the target geometry was optimized for both irradiation and dissolution. For theoretical irradiation, a low W-density metallic target is optimal for W-188 production, as discussed in section 1.1.2. The global geometry of these targets were found to be macroporous, with a porosity of around 20-27%. Coarse W powder with particle sizes up to 100 $\mu$ m are optimal for creating pores in the final compact. Compacts made with 4 tons of pressure and 2hrs of annealing at 1750°C was sufficient to hold the pellets together. However, the particle interfaces in the pellet did not show sufficient bonding and would create a potential hazard if the pellet fell apart. Compacts made with 6 tons of pressure and 24hrs of annealing created compacts with sufficient bonding between the particles while keeping the porosity of the material intact. Increasing the anneal time or force during compaction would decrease the porosity and would not be favorable for isotope production.

For the chemical processing of these targets, the porosity enhanced its ability to dissolve. As demonstrated here, these 2.2g tungsten targets were able to be dissolved within 90 minutes. By comparison, it is reported that dissolving a sintered tungsten ring takes longer than 3 hours [4] and may not be complete. The fact that the initial material was a powder and not a near theoretical dense piece of tungsten was advantageous when the target completed stage 1 of the dissolution process, leaving a powder to interact with for stage 2. Given the fact that stage 2 (Figure 7B) of the dissolution process led to vigorous boiling, it is still advised to have an OsO<sub>4</sub> scrubbing array, to prevent Os from escaping into the environment. The coproduction of Os191 with the W188 product is inevitable during the reactor irradiation of the W186 target. As long as the formation of volatile OsO<sub>4</sub>-191 is constrained, it may be possible to minimize Os191 release.

### 4.2 Recommendations

In this study, only cold and un-irradiated W-metal targets were fabricated and dissolved. A follow-up study incorporating Re and Os would be needed to evaluate the strategy provided here. As an initial study, Re and Os could be added to the compact to study its interaction with hydrogen peroxide. However, in irradiated W-metal targets, Re- and Os form precipitates [5-7]. The interaction of these precipitates with peroxides may be different than Re and Os alone. Therefore, irradiated W-metal samples should be studied directly.

In addition to studying irradiated W-metal targets, their subsequent purification and evaluation of the eluate should be examined. As the dissolution of these targets had residual W (Table 3), it would be important to extend the dissolution time and ensure that no W breakthrough occurs.

## 5 CITATION

1. Dash, A. and F.R. Knapp Jr, *An overview of radioisotope separation technologies for development of  $^{188}\text{W}/^{188}\text{Re}$  radionuclide generators providing  $^{188}\text{Re}$  to meet future research and clinical demands*. RSC Advances, 2015. 5(49): p. 39012-39036.
2. Martinho, E., J. Salgado, and I. Gonçalves, *Universal curve of the thermal neutron self-shielding factor in foils, wires, spheres and cylinders*. Journal of Radioanalytical and Nuclear Chemistry, 2004. 261: p. 637-643.
3. Boschi, A., et al.,  *$^{188}\text{W}/^{188}\text{Re}$  generator system and its therapeutic applications*. Journal of chemistry, 2014. 2014.
4. Du, M., *The Recovery of Medical Isotopes  $^{188}\text{W}$  from Irradiated W Metal Target - A New Approach*, in Oak Ridge National Laboratory. 2023: Oak Ridge, TN 37831.
5. Tanno, T., et al., *Effects of transmutation elements on neutron irradiation hardening of tungsten*. Materials Transactions, 2007. 48(9): p. 2399-2402.
6. Suzudo, T., M. Yamaguchi, and A. Hasegawa, *Migration of rhenium and osmium interstitials in tungsten*. Journal of Nuclear Materials, 2015. 467: p. 418-423.
7. Dürschnabel, M., et al., *New insights into microstructure of neutron-irradiated tungsten*. Scientific reports, 2021. 11(1): p. 7572.